ChemComm

Effect of polar amino acid incorporation on Fmoc-diphenylalanine-based tetrapeptides

Journal:	*ChemComm*
Manuscript ID	CC-COM-12-2019-009677
Article Type:	Communication

ChemComm
Chemical Communications

Guidelines for Referees

Thank you very much for agreeing to review this manuscript for *ChemComm*.

ChemComm is the Royal Society of Chemistry's most cited journal, and has a long history of publishing exciting new findings of exceptional significance, across the breadth of chemistry.

Communications should be urgent and of very high significance and interest to their field.

ChemComm's Impact Factor is **6.164** (2018 Journal Citation Reports®)

The following manuscript has been submitted for consideration as a

COMMUNICATION

For acceptance, a Communication must report new, primary research that is of high urgency warranting rapid publication. The topic of the manuscript should be of very high significance and interest to experts in the field, while also highlighting its wide appeal to the journal's general chemistry readership.

Articles which rely excessively on supplementary information for key information are more suited to a full paper format and are not suitable for *ChemComm*.

We ask referees to **recommend only work that is of a very high quality and novelty standard** for publication in *ChemComm*. When making your recommendation please:

- **Comment on** the novelty and significance to the field, and scientific reliability.
- **Note that routine or incremental** work should not be recommended for publication in *ChemComm*.
- **Comment if the author** has not provided fully convincing evidence for the homogeneity, purity and identity of all compounds they claim as new, in line with our guidelines.
- **Contact the Editor** if there is any conflict of interest, if the work has been previously published or if there is a significant part of the work which you are not able to referee with confidence.

Best regards,

Professor Véronique Gouverneur
Editorial Board Chair
University of Oxford

Dr Richard Kelly
Executive Editor
Royal Society of Chemistry

Contact us

Please visit our reviewer hub for further details of our processes, policies and reviewer responsibilities as well as guidance on how to review, or click the links below.

What to do when you review

Reviewer responsibilities

Process & policies

DEMENTIA RESEARCH CENTRE
Faculty of Medicine and Health Sciences

MACQUARIE University
SYDNEY·AUSTRALIA

13 December 2019

Professor Veronique Gouverner
Editorial Chair
Chemical Communications

Dear Professor Gouverner,

My colleagues and I are pleased to submit our manuscript entitled "**Effect of polar amino acid incorporation on Fmoc-diphenylalanine-based tetrapeptides**" for publication in *Chemical Communications*.

Here, we show that the incorporation of polar amino acids bearing positive, negative or no charge into the widely used Fmoc-diphenylalanine short peptide motif has significant effects on peptide self-assembly and function. Through comprehensive characterisation we show that these polar tetrapeptide hydrogels display differences in hydrogel stiffness (across three orders of magnitude) and nanoscale morphology. We validate that the incorporation of polar, charged amino acids imparts an electrostatic charge onto the tetrapeptide which is conserved throughout the solution and gel state. This charge greatly affects the biocompatibility of these tetrapeptides in both the solution and gel state, with cytotoxic tetrapeptides in the solution state being well tolerated in the gel state, and vice versa. Finally, we gain insights these biocompatibility trends through tethered bilayer lipid membrane (tBLM) experiments, which confirm interactions of positively charged tetrapeptides with cell-mimetic membranes.

To the best of our knowledge, our report is the first to show that *differences in biocompatibility depend not only the electrostatic charge of the peptides, but also the manner in which peptide biocompatibility is evaluated*. Many papers, when assessing the biocompatibility of self-assembling peptides, use a solution cytotoxicity assay (i.e. treating a monolayer of cells with peptides at well below their critical gel concentration). In this work, we show that peptides which demonstrate excellent biocompatibility as determined through this method are unable to support cells in the gel state, owing to a lack of attachment. We further show that there is no relationship between hydrogel stiffness and biocompatibility for these tetrapeptide hydrogels.

Our work illustrates the importance of electrostatic charge on peptide self-assembly and biocompatibility, and that the method used to evaluate biocompatibility is reflective of the intended applications of these materials. This work has applications in tissue engineering, supramolecular chemistry and biochemistry. Thus, we believe that our work is well-suited for the broad readership of *Chemical Communications*, and will attract readers from across supramolecular chemistry, biomaterials, and tissue engineering communities to the journal.

We are looking forward to your and the reviewer's comments and please do not hesitate to contact us if you require further information.

Sincerely,
Dr Adam Martin

DR ADAM D MARTIN
Senior Research Fellow, Group Leader

Macquarie University
NSW 2109 Australia
T: +61 (2) 9850 2671
M: +61 452 440 155
E: adam.martin@mq.edu.au

ABN 90 952 801 237 | CRICOS Provider 00002J

MACQUARIE University
SYDNEY·AUSTRALIA

DR ADAM D MARTIN
Senior Research Fellow, Group Leader

Macquarie University
NSW 2109 Australia

T: +61 (2) 9850 2671
M: +61 452 440 155

E: adam.martin@mq.edu.au

Journal Name

COMMUNICATION

Effect of polar amino acid incorporation on Fmoc-diphenylalanine-based tetrapeptides

Received 00th January 20xx,
Accepted 00th January 20xx

DOI: 10.1039/x0xx00000x

www.rsc.org/

A. Daryl Ariawan,[a] Biyun Sun,[a] Jonathan P. Wojciechowski,[b] Ian Lin,[c] Eric Y. Du,[c] Sophia C. Goodchild,[d] Charles G. Cranfield,[e] Lars M. Ittner,[a] Pall Thordarson,[c] Adam D. Martin*[a]

Peptide hydrogels show great promise as extracellular matrix mimics due to their tuneable, fibrous nature. Through incorporation of polar, charged amino acids into the Fmoc-diphenylalanine motif, we show that electrostatic charge plays a key role in the self-assembly and biocompatibility of these peptides in both the sol and gel state.

Since the diphenylalanine sequence was first reported to self-assemble into nanotubes,[1] it has been the basis for a wealth of research, ranging from electronically responsive materials,[2,3] to sensors,[4,5] to cell scaffolds.[6,7] The addition of the amine-protecting Fmoc moiety to the N-terminus of diphenylalanine results in the self-assembly of nanofibres under aqueous conditions, yielding self-supporting hydrogels.[8] These hydrogels or derivatives thereof have since provided a number of elegant examples of self-assembly; to support different cell types,[9-11] deliver therapeutic cargo[12,13] or even selectively destroy cancerous cells.[14] As the Fmoc-diphenylalanine (Fmoc-FF) sequence itself does not promote cell adhesion, the integrin binding motif arginine-glycine-aspartic acid (RGD) has been either attached to, or co-assembled with Fmoc-FF to improve cell viability.[15,16] It has been shown that even co-assembling Fmoc-3F-Phe-Arg-OH and Fmoc-3F-Phe-Asp-OH has a synergistic effect on fibroblast growth.[17]

In addition to the RGD sequence, other epitopes, typically laminin and collagen-based, have promoted cell adhesion in peptide hydrogels.[18-21] Recent work has shown that the spacing between adjacent cell adhesive epitopes is important for the adhesion of endothelial cells.[22] Although control over epitope incorporation and spacing throughout a scaffold is useful for enhancing adhesion, in many cases the surface presentation of the desired peptide sequence is unknown.

One strategy which has been widely applied in the polymer hydrogel field is to replace cell adhesive epitopes with electrostatic charge.[23-25] A positively charged scaffold interacts favourably with the negatively charged cell membrane, resulting in enhanced adhesion. This has been applied to peptide hydrogels through the co-assembly of non-gelators Fmoc-lysine (Fmoc-K) or poly-lysine with Fmoc-FF scaffolds.[26,27] Surprisingly, relatively little work has been undertaken on the incorporation of charged residues into self-assembling peptide sequences, with the exception of the pioneering work on octapeptides bearing complementary charges.[28,29] The incorporation of positively charged lysine or ornithine at the C-terminus of Fmoc-FF has been reported, however the ability of these peptides to support cell growth was not established.[30]

Herein we have inserted the polar anionic amino acids aspartic acid (D) and glutamic acid (E), polar neutral amino acids asparagine (N) and glutamine (Q), and polar cationic amino acids arginine (R) and lysine (K) at the N-terminus of the diphenylalanine self-assembling sequence. All six tetrapeptides give self-supporting hydrogels. Zeta potential measurements show that the electrostatic charge imparted by the incorporation of polar amino acids is maintained in the gel state, and the biocompatibility of these charged tetrapeptides is evaluated in both the solution and gel state.

The Fmoc-diphenylalanine sequence was used as a starting point for the design of the peptides examined in this study, as its self-assembly has been well established.[8] We inserted polar amino acids at the N-terminus of the peptide, ensuring that the diphenylalanine sequence was conserved (Fig. 1). Charged amino acids were inserted at the N-terminus of the peptide to minimise chances of the peptide C-terminus forming dimers with acidic residues (D, E), or salt bridges with cationic residues (R, K). Tripeptides containing a single polar amino acid were also synthesised, however cationic tripeptides Fmoc-RFF

[a] Dementia Research Centre, Department of Biomedical Science, Faculty of Medicine and Health Sciences, Macquarie University, Sydney, NSW 2109, Australia.
[b] Department of Materials, Imperial College London, Exhibition Road, London SW7 2AZ, United Kingdom.
[c] School of Chemistry, The Australian Centre for Nanomedicine and the ARC Centre for Convergent Bio-Nano Science & Technology, University of New South Wales, Sydney, NSW, 2052, Australia.
[d] Department of Molecular Sciences, Faculty of Science and Engineering, Macquarie University, Sydney, NSW 2109, Australia.
[e] School of Life Sciences, University of Technology Sydney, Ultimo, NSW 2007, Australia.

Electronic Supplementary Information (ESI) available: Experimental details including synthesis and characterisation of peptides and peptide hydrogels. See DOI: 10.1039/x0xx00000x

and Fmoc-KFF were insoluble in aqueous media, possibly due to their zwitterionic nature.

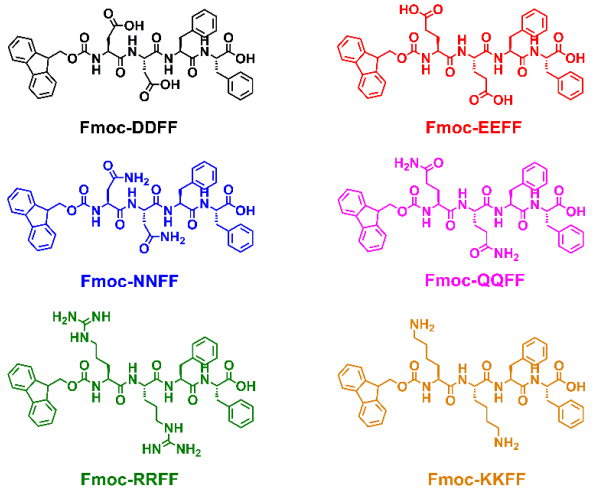

Fig. 1 – The Fmoc tetrapeptides which were synthesised for this study, featuring insertion of (top) polar anionic, (middle) polar neutral and (bottom) polar cationic amino acids inserted at the N-terminal end of the diphenylalanine sequence.

All tetrapeptides self-assembled into hydrogels. For anionic Fmoc-DDFF and Fmoc-EEFF, gelation was accomplished using a pH switch employing glucono-δ-lactone (GdL),[31] with these peptides having minimum gel concentrations (mgc) of 0.05% and 0.25% (w/v), respectively (Fig. S2a, b). For polar neutral tetrapeptides Fmoc-NNFF and Fmoc-QQFF the GdL pH switch mechanism yielded hydrogels with mgc values of 0.25% and 0.10% (w/v), respectively (Fig. S2c, d). Polar cationic tetrapeptides Fmoc-RRFF and Fmoc-KKFF were water soluble, and addition of acid served only to enhance their solubility. Heterogeneous hydrogels were obtained through the addition of dilute base (NaOH), however, the addition of an ionic solution (*i.e.* cell culture media) gave homogenous hydrogels with an mgc of 0.5% (w/v) for both Fmoc-RRFF and Fmoc-KKFF (Fig. S2e, f).

Atomic force microscopy (AFM) imaging of hydrogels shows the presence of nanofibres for anionic (Fmoc-DDFF, Fmoc-EEFF), and cationic (Fmoc-RRFF, Fmoc-KKFF) tetrapeptides, however, for neutral tetrapeptides Fmoc-NNFF and Fmoc-QQFF, globular aggregates are observed, potentially suggesting a different self-assembly mechanism (Fig. 2). Distinct right-handed fibres of Fmoc-EEFF can be observed (Fig. 2b, pitch approximately 35 nm). Fibre diameters ranged from 2.8 ± 1.1 nm for Fmoc-KKFF to 6.5 ± 1.1 nm for Fmoc-EEFF (Table S1). No trends relating to fibre diameter and peptide charge were observed.

The secondary structure of the peptides was assessed through a combination of circular dichroism (CD) and attenuated total reflectance infrared spectroscopy (ATR-IR). The parent Fmoc-FF peptide is known to self-assemble into β-sheets, yielding a strong absorbance at approximately 220 nm.[32] This is also the case for Fmoc-DDFF, with Fmoc-NNFF, Fmoc-QQFF and Fmoc-KKFF giving slightly shifted absorption maxima (215 nm) which indicate β-sheet formation (Fig. S3). Alternately, Fmoc-EEFF and Fmoc-RRFF show a shifted maximum at 230 nm. ATR-IR spectra confirm β-sheet formation for all peptides (Fig. S4), with every tetrapeptide displaying an absorption between 1630 – 1640 cm^{-1}.[33,34]

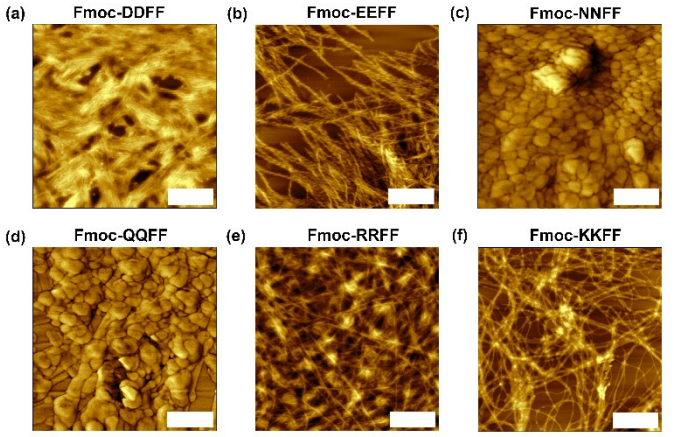

Fig. 2 – Atomic force microscopy images of each tetrapeptide, showing self-assembly into fibres in the case of (a, b) polar anionic and (e, f) polar cationic tetrapeptides and (c, d) globular aggregates for polar neutral tetrapeptides. Samples were prepared through spread coating at 0.05% (w/v) onto freshly cleaved mica, scale bar represents 500 nm for a, e and f, and 300 nm for b, c and d.

We evaluated the mechanical properties of the hydrogels formed by each polar tetrapeptide (Fig. 3a, Fig S5-S10) through rheology at concentrations of 1, 0.5 and 0.25% (w/v), as these were the concentrations used for contact cytotoxicity. The rheology of Fmoc-RRFF and Fmoc-KKFF was not studied at 0.25% (w/v), as this fell below their mgc. As expected, hydrogel stiffness increased with concentration for all tetrapeptide hydrogels. Anionic tetrapeptide Fmoc-DDFF gave the stiffest hydrogels, likely owing to formation of fibre bundles (Fig. 2a), as bundle size is proportional to hydrogel stiffness.[35] The large difference in stiffness between Fmoc-NNFF and Fmoc-QQFF is due to the propensity of Fmoc-QQFF to aggregate over time, with this metastability adversely affecting its mechanical properties. Polar cationic tetrapeptides Fmoc-RRFF and Fmoc-KKFF gave softer hydrogels, due to the use of a salt screen method to trigger gelation, this tends to "freeze in" the fibre structure,[36] compared to the slow hydrolysis of GdL which allows for evolution of hierarchical networks.

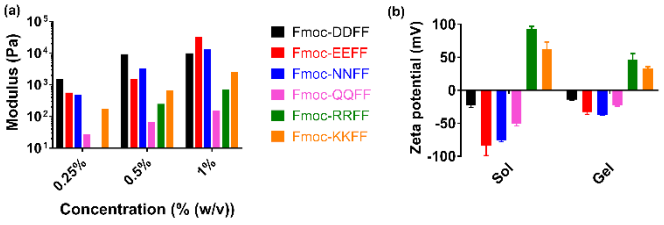

Fig. 3 – Characterisation of polar tetrapeptide hydrogels. (a) Storage modulus of tetrapeptide hydrogels at concentrations relevant to cytotoxicity studies, showing storage moduli which span several orders of magnitude dependent on peptide sequence. (b) Zeta potential of polar tetrapeptides in both the sol and gel state, showing the expected positive and negative charges for each peptide, which is then reduced upon gelation. Error bars represent standard deviation from the mean.

Next, the pK_a of each peptide was determined (Fig S11). The pK_a of Fmoc-FF is approximately 7,[37] and that the addition of aspartic acid groups lowers pK_a values.[38] This is also observed for our peptides, with Fmoc-DDFF having a pK_a of 4.8 and Fmoc-EEFF a pK_a of 6.2. This agrees with the lower pK_a of aspartic acid relative to glutamic acid (3.65 *versus* 4.25, respectively). Fmoc-KKFF yielded a pK_b of 11.1, and Fmoc-RRFF a pK_b of 11.2, suggesting that in this case, the nature of the cationic amino acid does not affect the peptide pK_b.

To show that the incorporation of polar, charged amino acids translates to the charged sols and hydrogels, zeta potentials were recorded for tetrapeptides in the sol and gel state (Fig. 3b). A negative zeta potential is observed for polar anionic and polar neutral tetrapeptides owing to the deprotonation of acidic residues required to solubilise the peptide. The polar cationic peptides Fmoc-RRFF and Fmoc-KKFF, which were dissolved in water, have positive zeta potentials. For all tetrapeptides, the charge observed for the peptide sol was reduced upon gelation yet remained negative (for polar anionic/neutral tetrapeptides) or positive (for polar cationic tetrapeptides). To confirm that the zeta potential results were not an artefact of the equilibrium between monomeric and self-assembled peptides, the cationic dye Rhodamine 6G, was incubated with hydrogels of Fmoc-DDFF and Fmoc-KKFF (Fig. S12, S13), and its release monitored over 24h. The amount of dye released is far greater for anionic Fmoc-DDFF than cationic Fmoc-KKFF, confirming that the tetrapeptides are indeed charged in the hydrogel state.

With the presence of electrostatic charge in both the sol and gel state established, the biocompatibility of these polar tetrapeptides in the sol and gel state was evaluated using the robust HEK-293T cell line. For solution cytotoxicity, tetrapeptides were prepared in cell culture media and added to a cell monolayer. In the solution state, all polar tetrapeptides except for Fmoc-RRFF are well tolerated up to 0.1% (w/v). Above this concentration, aggregation effects start to occur for Fmoc-EEFF and Fmoc-QQFF, resulting in cytotoxicity.[39] Fmoc-RRFF is cytotoxic at low concentrations (> 0.01% (w/v)), due to its ability to interact with cell membranes.

Interestingly, the cytotoxicity of the polar tetrapeptides in the gel state shows an inverse correlation to that observed in the solution state, for anionic and cationic tetrapeptides. Fmoc-DDFF and Fmoc-EEFF show dramatically decreased cell viability, and Fmoc-RRFF and Fmoc-KKFF increased viability, with these trends especially evident at 1% (w/v). Polar neutral tetrapeptides Fmoc-NNFF and Fmoc-QQFF showed excellent viability across all concentrations. It should be noted that there is no apparent correlation between peptide mechanical properties (Fig. 3a) and biocompatibility (Fig. 4).

We hypothesise that negatively charged peptides, such as Fmoc-DDFF and Fmoc-EEFF have limited interactions with the negatively charged cell membrane. Whilst this gives good biocompatibility when treating adherent cells with peptide solutions (Fig. 4a), cells do not adhere to scaffolds composed of these peptides, decreasing cell viability (Fig. 4b). Alternately, positively charged Fmoc-KKFF and Fmoc-RRFF can interact with the cell membrane, potentially resulting in reduced viability in the solution state (as observed for Fmoc-RRFF), however in the gel state this attractive interaction between the cell membrane and hydrogel scaffold results in cell adherence and viability. Polar neutral tetrapeptides Fmoc-NNFF and Fmoc-QQFF will not exhibit electrostatic-mediated interactions with the cell membrane, which translates to good cell viability in both the solution and gel state.

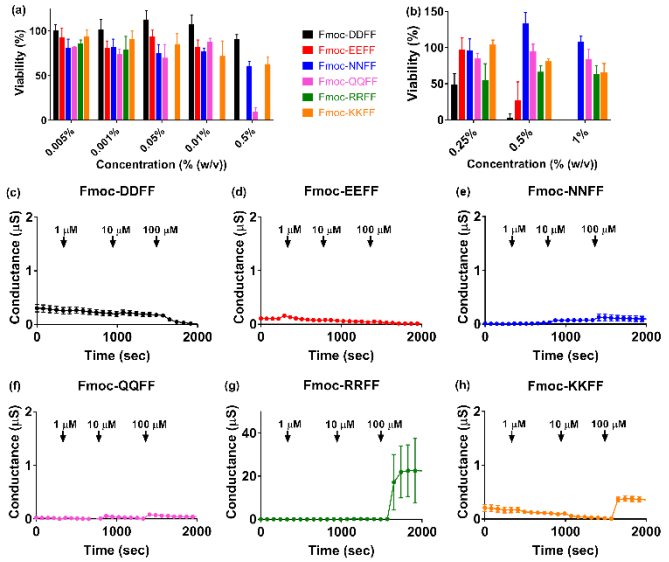

Fig. 4 – Cytotoxicity of polar peptides towards HEK293T cells in (a) the solution state and (b) the gel state. Interestingly, many of the trends observed in the solution cytotoxicity assay are inverted in the gel state cytotoxicity measurements. (c-h) Tethered bilayer lipid membrane permeability measurements showing that polar cationic peptides (g) Fmoc-RRFF and (h) Fmoc-KKFF have the ability to interact with cell membranes.

To validate this hypothesis, we treated sparsely tethered lipid bilayer membranes (tBLMs) consisting of 1-Palmitoyl-2-oleoylphosphatidylcholine (POPC) lipids with tetrapeptides and monitored electrical impedance over time. These cell-mimetic membranes have been used previously to assess the membrane disruptive activity of peptides.[40-42] For polar anionic and polar neutral tetrapeptides, no interaction with the tBLMs were observed at all concentrations (Fig. 4c-f). Polar cationic peptides showed interactions with the tBLMs at 100 μM (Fig. 4g, h), which is equivalent to approximately 0.02% (w/v). Fmoc-RRFF, in particular, shows a 50-fold increase in conductance relative to Fmoc-KKFF, suggesting a major disruption to the tBLM. Interestingly, this is exactly where the tetrapeptide begins to show cytotoxic effects in the solution state. The interactions of arginines with cell membranes are known and form the basis of many cell penetrating peptides including the TAT sequence, penetratin and oligoarginines.[43]

In conclusion, we have examined the effect of incorporating polar amino acids aspartic acid, glutamic acid, asparagine, glutamine, arginine and lysine into the Fmoc diphenylalanine self-assembling sequence, yielding cationic, neutral or anionic tetrapeptides. These polar amino acids affect both the mechanical properties and the nanoscale morphology of the resultant peptides. Zeta potential measurements in the sol and gel state show that anionic and

neutral peptides retain a negative charge due to the deprotonation of their acidic residues and C-terminus; whilst cationic tetrapeptides bear a positive charge. The biggest differences between these polar tetrapeptides is in their cytotoxicity, with anionic tetrapeptides Fmoc-DDFF and Fmoc-EEFF being biocompatible when applied to cells in the solution state but cytotoxic in the gel state. The opposite trend is observed for cationic tetrapeptides Fmoc-RRFF and Fmoc-KKFF, with Fmoc-RRFF being especially cytotoxic in the solution state, but both peptides being well-tolerated in their gel state. Polar neutral tetrapeptides Fmoc-NNFF and Fmoc-QQFF exhibited good biocompatibility in both the solution and gel state. This work highlights the important role that electrostatic interactions play when designing short peptide hydrogels for cell scaffolding applications, which will undoubtedly prove useful for the future rational design of these materials.

Acknowledgements

We would like to thank the Mark Wainwright Analytical Centre (UNSW) and Professor Alison Rodger (Macquarie University) for access to instruments. Aspects of this research have been facilitated by access to the Australian Proteome Analysis Facility supported under the Australian Government's National Collaborative Research Infrastructure Strategy (NCRIS). We acknowledge the Australian Research Council for Discovery Project grants (DP130101512 and DP190101892) and an ARC Centre of Excellence grant (CE140100036) to PT and Discovery Project grants (DP170100781 and DP170100843) to LI. We also acknowledge the National Health and Medical Research Council for a Dementia Research Fellowship (1106751) to ADM, and project grants (1081916 and 1132524) and an NHMRC Principal Research Fellowship (1123564) to LI. We would like to thank the Australian Government for APAs awarded to JPW.

Referencess

1 M. Reches and E. Gazit, *Science*, 2003, **300**, 625-627.
2 K. Tau, P. Makam, R. Aizen and E. Gazit, *Science*, 2017, **358**, eeam9578.
3 V. Nguyen, R. Zhu, K. Jenkins and R. Yang, *Nat. Commun.*, 2016, **7**, 13566.
4 M. Reches and E. Gazit, *Nat. Nanotechnol.*, 2006, **1**, 195-200.
5 R. de la Rica and H. Matsui, *Chem. Soc. Rev.*, 2010, **39**, 3499-3509.
6 K. Tao, A. Levin, L. Adler-Abramovich and E. Gazit, *Chem. Soc. Rev.*, 2016, **45**, 3935-3953.
7 E. R. Draper and D. J. Adams, *Chem*, 2017, **3**, 390-410.
8 M. Reches and E. Gazit, *Isr. J. Chem.*, 2005, **45**, 363-371.
9 K. F. Bruggeman, Y. Wang, F. L. Maclean, C. L. Parish, R. J. Williams and D. R. Nisbet, *Nanoscale*, 2017, **9**, 13661-13669.
10 L. A. Castillo-Diaz, M. Elsawy, A. Saiani, J. E. Gough and A. F. Miller, *J. Tissue Eng.*, 2016, **7**, 1-15.
11 J. Zhou, X. Du, C. Berciu, H. He, J. Shi, D. Nicastro and B. Xu, *Chem*, 2016, **1**, 246-263.
12 V. M. P. Viera, L. L. Hay and D. K Smith, *Chem. Sci.*, 2017, **8**, 6981-6990.
13 J. Zhou, J. Li, X. Du and B. Xu, *Biomaterials*, 2017, **129**, 1-27.
14 Z. Feng, H. Wang, X. Chen and B. Xu, *J. Am. Chem. Soc.*, 2017, **139**, 15377-15384.
15 M. Zhou, A. M. Smith, A. K. Das, N. W. Hodson, R. F. Collins, R. V. Ulijn and J. E. Gough, *Biomaterials*, 2009, **30**, 2523-2530.
16 V. Castelletto, I. W. Hamley, C. Stain and C. Connon, *Langmuir*, 2012, **28**, 12575-12580.
17 W. Liyanage, K. Vats, A. Rajbhandary, D. S. W. Benoit, B. L. Nilsson, *Chem. Commun.*, 2015, **51**, 11260-11263.
18 A. L. Rodriguez, C. L. Parish, D. R. Nisbet and R. J. Williams, *Soft Matter*, 2013, **9**, 3915-3919.
19 W. Wang, J. Hu, M. Zheng, L. Zheng, H. Wang and Y. Zhang, *Org. Biomol. Chem.*, 2015, **13**, 11492-11498.
20 Md. M. Hassan, A. D. Martin, P. Thordarson, *ChemPlusChem*, 2018, **83**, 47-52.
21 G. A. Silva, C. Czeisler, K. L. Niece, E. Beniash, D. A. Harrington, J. A. Kessler and S. I. Stupp, *Science*, 2004, **303**, 1352-1355.
22 E. T. Pashuck, B. J. R. Duche, C. S. Hansel, S. A. Maynard, L. W. Chow and M. M. Stevens, *ACS Nano*, 2016, **10**, 11096-11104.
23 C. Sinthuvanich, L. A. Haines-Butterick, K. J. Nagy and J. P. Schneider, *Biomaterials*, 2012, **33**, 7478-7488.
24 S. N. Pawar and K. J. Edgar, *Biomaterials*, 2012, **33**, 3279-3305.
25 H. Li and J. J. Cooper-White, *Biomater. Sci.*, 2014, **2**, 1693-1705.
26 R. Xing, S. Li, N. Zhang, G. Shen, H. Mohwald and X. Yan, *Biomacromolecules*, 2017, **18**, 3514-3523.
27 V. Jayawarna, S. M. Richardson, A. R. Hirst, N. W. Hodson, A. Saiani, J. E. Gough and R. V. Ulijn, *Acta Biomater.*, 2009, **5**, 934-943.
28 D. Roberts, C. Rochas, A. Saiani, A. F. Miller, *Langmuir*, 2012, **28**, 16196-16206.
29 J. Gao, C. Tang, M. Elsawy, A. M. Smith, A. F. Miller, A. Saiani, *Biomacromolecules*, 2017, **18**, 826-834.
30 A. P. McCloskey, E. R. Draper, B. F. Gilmore, G. Laverty, *J. Pept. Sci.*, 2017, **23**, 131-140
31 D. J. Adams, M. F. Butler, W. J. Frith, M. Kirkland, L. Muller and P. Sanderson, *Soft Matter*, 2009, **5**, 1856-1862.
32 A. M. Smith, R. J. Williams, C. Tang, P. Coppo, R. F. Collins, M. L. Turner, A. Saiani and R. V. Ulijn, *Adv. Mater.*, 2008, **20**, 37-41.
33 S. Fleming, S. Debnath, P. W. J. M. Frederix, T. Tuttle and R. V. Ulijn, *Chem. Commun.*, 2013, **49**, 10587-10589.
34 S. Fleming, P. W. J. M. Frederix, I. R. Sasselli, N. T. Hunt, R. V. Ulijn and T. Tuttle, *Langmuir*, 2013, **29**, 9510-9515.
35 P. J. H. Kouwer, M. Koepf, V. A. A. Le Sage, M. Jaspers, A. M. van Buul, Z. H. Eksteen-Akeroyd, T. Woltinge, E. Scwartz, H. J. Kitto, R. Hoogenboom, S. J. Picken, R. J. M. Nolte and A. E. Rowan, *Nature*, 2013, **493**, 651-655.
36 L. Chen, G. Pont, K. Morris, G. Lotze, A. Squires, L. C. Serpell, D. J. Adams, *Chem. Commun.*, 2011, **47**, 12071-12073.
37 C. Tang, A. M. Smith, R. F. Collins, R. V. Ulijn, A. Saiani, *Langmuir*, 2009, **25**, 9447-9453.
38 A. L. Rodriguez, C. L. Parish, D. R. Nisbet, R. J. Williams, *Soft Matter*, 2013, **9**, 3915-3919.
39 W. T. Truong, Y. Su, D. Gloria, F. Braet, P. Thordarson, *Biomater. Sci.*, **3**, 2015, 298-307.
40 T. Berry, D. Dutta, R. Chen, A. Leong, H. Wang, W. A. Donald, M. Parviz, B. Cornell, M. Wilcox, N. Kumar, C. G. Cranfield, *Langmuir*, **34**, 2018, 11586-11592.
41 Z. Su, J. J. Leitch, R. J. Faragher, A. L. Schwan, J. Lipkowski, *Electrochim. Acta*, **243**, 2017, 364-373.
42 C. G. Cranfield, S. T. Henriques, B. Martinac, P. Duckworth, D. J. Craik, B. Cornell, *Langmuir*, **33**, 2017, 6630-6637.
43 G. Guidotti, L. Brambilla, D. Rossi, *Trends Pharamcol. Sci.*, **38**, 2017, 406-424.

Supplementary information

Charge mediated biocompatibility in peptide hydrogel scaffolds

A. Daryl Ariawan,[a] Biyun Sun,[a] Jonathan P. Wojciechowski,[b] Ian Lin,[c] Eric Y. Du,[c] Sophia C. Goodchild,[d] Charles G. Cranfield,[e] Lars M. Ittner,[a] Pall Thordarson,[c] Adam D. Martin*[a]

[a] Dementia Research Centre, Department of Biomedical Science, Faculty of Medicine and Health Sciences, Macquarie University, Sydney, NSW 2109, Australia.

[b] Department of Materials, Imperial College London, Exhibition Road, London SW7 2AZ, United Kingdom.

[c] School of Chemistry, The Australian Centre for Nanomedicine and the ARC Centre for Convergent Bio-Nano Science & Technology, University of New South Wales, Sydney, NSW, 2052, Australia.

[d] Department of Molecular Sciences, Faculty of Science and Engineering, Macquarie University, Sydney, NSW 2109, Australia.

[e] School of Life Sciences, University of Technology Sydney, Ultimo, NSW 2007, Australia.

Contents:

Solid phase peptide synthesis of capped dipeptides

Initial amino acid loading

2-chlorotrityl chloride resin (100-200 mesh; 1% DVB; 1.1 mmol/g) (500 mg, 0.55 mmol) was weighed into a 10 mL polypropylene syringe equipped with a porous polypropylene frit (Torviq SF-1000), which was used as the reaction vessel. The resin was washed with dichloromethane (3 × 5 mL) before being allowed to swell in dichloromethane (5 mL) for at least 0.5 h prior to the loading of the first amino acid.

A solution of Fmoc-Phe-OH (3 equiv., 640 mg) was dissolved in a mixture of dry dichloromethane (2 mL), *N,N*-dimethylformamide (2 mL) and *N,N*-diisopropylethylamine (DIPEA) (8 equiv., 0.8 mL) and taken up into the syringe with resin and stirred overnight using an orbital shaker. The resin was then washed with dichloromethane (3 x 4mL) and *N,N*-dimethylformamide (DMF) (3 × 4 mL).

N-terminal Fmoc deprotection

A solution of 20% (v/v) piperidine in DMF (2 × 4 mL) was added to the resin once for 1 min, then a fresh aliquot was taken up again and stirred for 10 mins. The solution was subsequently expelled and the resin washed with DMF (5 × 4 mL). The resulting resin-bound amine was used immediately in the next peptide coupling step.

Amino acid coupling

The next amino acid (3 equiv., masses as below) was dissolved in a 0.45 M DMF solution of 1-hydroxybenzotriazole hydrate (HOBt·H_2O)/*N*,*N*,*N*′,*N*′-tetramethyl-*O*-(1H-benzotriazol-1-yl)uronium hexafluorophosphate (HBTU) (3 equiv.) and DIPEA (6 equiv., 0.6 mL) and this coupling solution added to the resin and stirred for 45 mins using an orbital shaker. The solution was expelled and the resin washed with DMF (5 x 4 mL).

Amino acid	Mass used (mg)
Fmoc-Phe-OH	640
Fmoc-Asp(O^{t}bu)-OH	680
Fmoc-Glu(O^{t}bu)-OH	702
Fmoc-Asn(Trt)-OH	984
Fmoc-Gln(Trt)-OH	1008
Fmoc-Arg(Pbf)-OH	1070
Fmoc-Lys(Boc)-OH	773

After another *N*-terminal Fmoc deprotection, iterative couplings were performed in order to build up the required peptide sequence.

Cleavage of the peptide

After the final coupling step, the resin was washed with DMF (3 x 4 mL) and dichloromethane (3 x 4 mL). For all peptides except Fmoc-NNFF, Fmoc-QQFF and Fmoc-RRFF, a solution of 1:9 dichloromethane: trifluoroacetic acid with three drops of water was then added to the resin, and the resin stirred for 2 hours using an orbital shaker. For Fmoc-NNFF and Fmoc-QQFF, the protected peptide was cleaved from the resin using 10% trifluoroacetic acid in dichloromethane and purified using semi-preparative HPLC, before lyophilisation and cleavage using 1:9 dichloromethane: trifluoroacetic acid and three drops of water for 2 hours. For Fmoc-RRFF, a solution of trifluoroacetic acid, water and triisopropylsilane in a 95: 2.5: 2.5 ratio was added to the resin and the resin stirred for 3h. The cleavage solution was then expelled, the resin washed with dichloromethane (2 x 4 mL) and the solvents evaporated under a stream of nitrogen. The resulting residue was lyophilised and purified by semi-preparative HPLC using an acetonitrile/water gradient, giving a white fluffy solid.

Characterisation data for **Fmoc-diaspartic acid-diphenylalanine (Fmoc-DDFF)**: IR: 3281 (m), 3064 (w), 3032 (w), 1703 (s), 1645 (s), 1534 (s), 1498 (m), 1448 (w), 1408 (w), 1260 (m), 1226 (s), 1192 (m), 1084 (w), 1049 (w), 916 (w), 739 (s), 699 (s); ^{1}H NMR (400 MHz, DMSO-d_6) δ 12.06 (br s, 1H), 8.20 (d, *J* = 7.2 Hz, 1H), 7.89 (d, *J* = 6.9 Hz, 1H), 7.76-7.66 (m, 2H), 7.41 (t, *J* = 7.0 Hz, 1H), 7.34-7.14 (m, 6H), 4.51 – 4.34 (m, 2H), 4.24 – 4.07 (m, 4H), 3.07-2.87 (m, 2H), 2.79 – 2.73 (m, 0.5H), 2.65-2.57 (m, 1H), 2.47-2.39 (m, 0.5H). ^{13}C NMR (101 MHz, DMSO-d_6) δ 173.08, 172.30, 172.25, 171.49, 171.05, 170.53, 156.31, 152.12, 151.75, 148.32, 148.16, 144.29, 141.19, 137.98, 137.84, 129.68, 129.61, 128.68, 128.46, 128.11, 127.57, 126.92, 125.81, 120.58, 54.18, 54.03, 50.07, 47.08, 37.79, 37.25, 36.37; HR-MS (ESI): calcd for $C_{41}H_{40}N_4O_{11}$ + Na^+: 787.2634, found 787.2679.

Characterisation data for **Fmoc-diglutamic acid-diphenylalanine (Fmoc-EEFF)**: IR: 3278 (m), 3065 (w), 3032 (w), 1697 (s), 1665 (m), 1636 (s), 1537 (s), 1498 (m), 1447 (m), 1404 (w), 1402 (w), 1286 (m), 1264 (s), 1219 (s), 1216 (s), 1104 (w), 1086 (w), 1041 (w), 914 (w), 785 (w), 760 (m), 741 (s), 697 (s); ^{1}H NMR (400 MHz, DMSO-d_6) δ 8.31 (d, *J* = 7.7 Hz, 1H), 7.99 (d, *J* = 8.2 Hz, 1H), 7.93–7.86 (m, 3H), 7.71 (t, *J* = 7.9 Hz, 2H), 7.56 (d, *J* = 8.0 Hz, 1H), 7.45–7.38 (m, 2H), 7.36–7.30 (m, 2H), 7.29–7.12 (m, 10H), 4.58–4.42 (m, 2H), 4.32–4.18 (m, 4H), 4.06–3.97 (m, 1H), 3.10–2.87 (m, 4H), 2.79–2.70 (m, 1H), 2.28–2.12 (m, 4H), 1.92–1.62 (m, 4H). ^{13}C NMR (126 MHz, DMSO-d_6) δ 174.50, 174.44, 173.12, 171.77, 171.34, 171.14, 156.43, 144.36, 144.18, 144.16, 137.95, 137.76, 129.58, 129.55, 128.66, 128.44, 128.12, 127.57, 126.91, 126.69, 125.77, 125.75, 120.58, 66.16, 54.34, 53.93, 53.86, 52.11, 47.11, 37.91, 37.16, 30.73, 30.46, 28.07, 27.68; HR-MS (ESI): calcd for $C_{43}H_{44}N_4O_{11}$ + Na^+: 793.3004, found 793.3087.

Characterisation data for **Fmoc-diasparagine-diphenylalanine (Fmoc-NNFF)**: IR: 3284 (m), 3067 (w), 1697 (m), 1643 (s), 1537 (s), 1442 (m), 1387 (w). 1321 (m), 1265 (s), 1200 (m), 910 (w), 740 (s), 696 (s); 1H NMR (400 MHz, DMSO-d_6) δ 8.14 (d, *J* = 7.5 Hz, 1H), 8.07 (d, *J* = 7.5 Hz, 1H), 7.95 (d, *J* = 8.1 Hz, 1H), 7.82 (d, *J* = 7.8 Hz, 2H), 7.67–7.60 (m, 2H), 7.50 (d, *J* = 7.8 Hz, 1H), 7.38–7.30 (m, 3H), 7.28–7.25 (m, 2H), 7.25–7.22 (m, 1H), 7.21–7.18 (m, 2H), 7.18–7.16 (m, 2H), 7.16–7.10 (m, 6H), 7.09–7.03 (m, 1H), 6.92 (s, 1H), 6.84 (s, 1H), 4.43–4.24 (m, 4H), 4.23–4.10 (m, 3H), 3.04–2.82 (m, 3H), 2.76–2.65 (m, 1H), 2.50–2.46 (m, 1H),

2.40–2.24 (m, 3H). 13C NMR (126 MHz, DMSO-d_6) δ 173.03, 172.11, 171.82, 171.19, 171.02, 156.21, 144.31, 144.25, 144.22, 141.14, 138.35, 137.97, 129.61, 129.57, 129.50, 128.83, 128.69, 128.51, 128.23, 128.11, 128.00, 127.60, 127.11, 126.89, 126.72, 126.62, 125.83, 120.56, 66.35, 56.23, 54.43, 54.16, 52.05, 50.41, 47.04, 37.95, 37.36, 37.24; HR-MS (ESI): calcd for $C_{41}H_{42}N_6O_9$ + Na^+: 763.3022, found 763.3097.

Characterisation data for **Fmoc-diglutamine-diphenylalanine (Fmoc-QQFF)**: IR: 3303 (m), 3066 (w), 1661 (s), 1637 (s), 1542 (s), 1444 (s), 1334 (w), 1270 (m), 1151 (m), 1010 (m), 755 (s), 698 (s); 1H NMR (400 MHz, DMSO-d6) δ 8.33 (d, *J* = 8.2 Hz, 1H), 7.98 (d, *J* = 7.9 Hz, 2H), 7.90 (d, *J* = 7.5 Hz, 2H), 7.72 (t, *J* = 7.5 Hz, 2H), 7.56 (d, *J* = 7.8 Hz, 1H), 7.42 (t, *J* = 7.5 Hz, 2H), 7.37–7.28 (m, 4H), 7.28–7.24 (m, 4H), 7.23–7.19 (m, 6H), 7.15–7.11 (m, 1H), 6.78 (d, *J* = 8.8 Hz, 2H), 4.57–4.40 (m, 2H), 4.29–4.18 (m, 4H), 4.01–3.93 (m, 1H), 3.11–2.88 (m, 3H), 2.81–2.68 (m, 1H), 2.18–1.95 (m, 4H), 1.91–1.60 (m, 4H). 13C NMR (126 MHz, DMSO-d6) δ 174.40, 174.29, 173.12, 171.96, 171.43, 171.36, 156.45, 144.35, 144.25, 144.22, 141.16, 137.96, 137.79, 129.57, 129.50, 128.82, 128.68, 128.47, 128.23, 128.12, 128.00, 127.58, 127.11, 126.92, 126.72, 125.80, 120.57, 66.22, 56.23, 54.87, 53.93, 52.51, 47.09, 37.95, 37.16, 32.06, 31.89, 28.70, 28.25; HR-MS (ESI): calcd for $C_{43}H_{46}N_6O_9$ + H^+: 791.3345, found 791.3408.

Characterisation data for **Fmoc-diarginine -diphenylalanine (Fmoc-RRFF)**: IR: 3288 (m), 3189 (m), 3066 (m), 2947 (w), 1664 (s), 1516 (s), 1451 (m), 1325 (w), 1254 (m), 1193 (s), 1182 (s), 1132 (s), 1032 (w), 837 (w), 801 (m), 759 (w), 741 (m), 721 (m), 699 (m); ^{1}H NMR (400 MHz, DMSO-d_6) δ 8.53 (s, 1H), 8.39 (d, *J* = 8.2 Hz, 1H), 8.22 (s, 1H), 7.87 (d, *J* = 7.9 Hz, 1H), 7.83 (d, *J* = 7.5 Hz, 2H), 7.64 (d, *J* = 7.5 Hz, 2H), 7.50 (d, *J* = 7.9 Hz, 1H), 7.41–7.32 (m, 3H), 7.30–7.22 (m, 3H), 7.20–7.13 (m, 7H), 7.13–7.06 (m, 8H), 4.27–4.18 (m, 2H), 4.17–4.08 (m, 3H), 4.03–3.96 (m, 1H), 3.93–3.86 (m, 1H), 3.09–3.02 (m, 1H), 3.00–2.90 (m, 4H), 2.90–2.81 (m, 2H), 2.72–2.63 (m, 1H), 1.65–1.49 (m, 2H), 1.46–1.11 (m, 6H). ^{13}C NMR (126 MHz, DMSO-d_6) δ 174.66, 171.86, 170.74, 163.72, 157.41, 157.28, 156.45, 144.27, 144.21, 144.18, 138.73, 138.38, 130.13, 129.38, 128.62, 128.29, 128.16, 127.55, 126.77, 126.46, 125.77, 125.73, 120.62, 66.11, 56.09, 55.51, 54.43, 52.96, 47.09, 41.14, 40.83, 37.99, 37.53, 30.50, 29.13, 25.19, 24.65; HR-MS (ESI): calcd for $C_{45}H_{54}N_{10}O_7$ - H^+: 845.4220, found 845.4105.

Characterisation data for **Fmoc-dilysine -diphenylalanine (Fmoc-KKFF)**: IR: 3286 (m), 3063 (m), 3034 (w), 2944 (m), 1663 (s), 1635 (s), 1524 (s), 1450 (m), 1412 (w), 1395 (m), 1334 (w), 1254 (m), 1201 (s), 1182 (s), 1130 (s), 1082 (w), 1032 (w), 837 (w), 800 (w), 757 (w), 739 (m), 722 (m), 697 (m); ^{1}H NMR (400 MHz, DMSO-d_6) δ 8.35 (d, *J* = 8.3 Hz, 1H), 7.90-7.87 (m, 4H), 7.72-7.69 (m, 3H), 7.42 (t, *J* = 7.8 Hz, 3H), 7.33 (t, *J* = 7.4 Hz, 2H), 7.25-7.15 (m, 10H), 4.37-4.13 (m, 6H), 3.96-3.91 (m, 1H), 3.09-2.89 (m, 4H), 2.76 – 2.64 (m, 5H), 1.58-1.17 (m, 12H). ^{13}C NMR (101 MHz, DMSO-d_6) δ 172.99, 170.92, 155.95, 143.79, 140.73, 138.25, 137.97, 129.53, 128.91, 128.07, 127.67, 127.07, 125.99, 125.28, 120.15, 65.54, 54.90, 54.16, 46.67, 37.47, 37.33, 32.77, 31.31, 27.12, 26.58, 22.45, 22.30; HR-MS (ESI): calcd for $C_{45}H_{54}N_6O_7$ + H^+: 791.4120, found 791.4196.

Preparation of hydrogels

pH switch

For Fmoc-DDFF, Fmoc-EEFF, Fmoc-NNFF and Fmoc-QQFF, 3.5 equivalents of 0.1 M aqueous sodium hydroxide was added to the peptide and milliQ water added to make the suspension up to the required concentration. This suspension was sonicated until homogenous, upon which time 4.5 molar equivalents of glucono-δ-lactone was added to lower the pH, resulting in gelation.

Salt screening

Fmoc-RRFF and Fmoc-KKFF were dissolved in milliQ water at the appropriate concentration, before an equal volume of Dulbecco's Modified Eagle Medium (DMEM) was added, to give the desired hydrogel concentration.

AFM measurements

Gel samples were prepared according to the appropriate gelation trigger described above and one drop of the hydrogel solutions was cast onto a freshly cleaved mica substrate, followed by spreading of the drop over the mica using a glass slide, with the excess liquid wicked away using capillary action. Samples were cast at 2x below their minimum gel concentration and left to dry in air overnight. Imaging was undertaken on a Bruker Multimode 8 atomic force microscope in Scanasyst mode in air, whereby the imaging parameters are constantly optimised through the force curves that are collected, preventing damage of soft samples. Bruker Scanasyst-Air probes were used, with a spring constant of 0.4 - 0.8 N/m and a tip radius of 2 nm.

Circular dichroism measurements

CD measurements for Fmoc-DDFF, Fmoc-EEFF, Fmoc-RRFF and Fmoc-KKFF were performed using a ChirascanPlus CD spectrometer, with data collected between wavelengths of 180 – 500 nm with a bandwidth of 1 nm, sample ratio of 0.1 s/point and step of 1 nm. CD measurements for Fmoc-NNFF and Fmoc-QQFF were collected on a Jasco J-1500 spectrophotometer, with data collected between 180 – 500 nm with a bandwidth of 2 nm, digital integration time (D.I.T.) of 2 seconds, scan speed of 100 nm/min and data pitch of 0.1 nm. In a typical experiment, 1% (w/v) peptide sols or hydrogels were prepared as above and diluted as necessary in water. Temperature was kept constant at 25 °C and all experiments were repeated at least three times and averaged into a single plot.

Attenuated Total Reflectance-Infrared Spectroscopy measurements

For Fmoc-DDFF, Fmoc-EEFF, Fmoc-RRFF and Fmoc-KKFF, fourier transform infrared spectroscopy (FTIR) measurements were made on a Perkin Elmer Spotlight 400 FT-IR spectrophotometer equipped with a diamond crystal attenuated total reflectance (ATR) accessory. For Fmoc-NNFF and Fmoc-QQFF, measurements were made on a JASCO FT/IR 4700 spectrophotometer fitted with a PIKE MIRacleTM Single Reflection ATR accessory and

ZnSe crystal plate. Hydrogels were prepared at 1% (w/v) in D_2O and pressed between the diamond crystal and substrate. All spectra were scanned at least 16 times over the range of 4000 - 650 cm^{-1} and were acquired at a resolution of 4 cm^{-1}.

Rheology measurements

Rheological measurements were performed on an Anton Paar MCR 302 rheometer using a 25 mm stainless steel parallel plate geometry configuration and analysed using RheoPlus v3.61 software. Typical rheology measurements involved casting 550 μL of a peptide hydrogel at the desired concentration, using the appropriate trigger described above, onto one of the stainless steel plates, lowering the other plate to the measurement position, and monitoring the storage and loss moduli over time. Once the storage modulus had plateaued, frequency sweep measurements were commenced. A Peltier temperature control hood and solvent trap was used to reduce evaporation and maintain a temperature of 25 °C for frequency and amplitude sweeps. Frequency sweeps were performed with a log ramp frequency (f) = 0.01 – 10 Hz and constant strain (γ) = 0.2%. Strain sweeps were performed with a log ramp strain (γ) = 0.1 – 100% at a constant frequency (f) = 1 Hz. Time resolved rheology was performed at constant frequency (f) = 1 Hz and strain (γ) = 0.2%. The rheology plots displayed are an average of at least three repeats for each point and error bars denote two standard deviations from the log-averaged mean.

pK_a measurements

Anionic and neutral polar tetrapeptides Fmoc-DDFF, Fmoc-EEFF, Fmoc-NNFF and Fmoc-QQFF were dissolved at a concentration of 0.1% (w/v) through the addition of MilliQ water and 3.5 equivalents of 0.1 M NaOH. 0.1 M HCl was added in 50 μL aliquots, and the pH allowed to stabilise for several minutes before a reading was taken. For cationic tetrapeptides Fmoc-RRFF and Fmoc-KKFF, 3.5 equivalents of 0.1 M HCl and MilliQ water were added to dissolve the peptide at 0.1% (w/v) and 0.1 M NaOH added in 50 μL aliquots. Each titration was repeated three times and averaged into a single plot. pK_a for Fmoc-DDFF and Fmoc-EEFF was determined to be the "buffering plateau" seen in Fig. S11, and pK_b was calculated by determining the volume at which the equivalence point occurs through plotting the derivative of the graph, finding the pH at half of this volume and subtracting from 14.

Zeta potential measurements

The zeta potential of peptide samples were measured using a Malvern Instruments Zetasizer NanoZS, equipped with a He-Ne laser beam with a wavelength of 633 nm and scattering angle of 12°. Measurements were performed in folded capillary cells (Malvern Instruments, DTS1070) using peptide sols prepared at 0.5% (w/v) (*i.e.* Fmoc-DDFF, Fmoc-EEFF, Fmoc-QQFF, Fmoc-NNFF dissolved in basic water and Fmoc-RRFF, Fmoc-KKFF dissolved in acidic water) and hydrogels prepared at 1% (w/v) (using a GdL trigger for Fmoc-DDFF, Fmoc-EEFF, Fmoc-NNFF and Fmoc-QQFF, and NaOH for Fmoc-RRFF and Fmoc-KKFF to avoid interference from buffer ions) which had then been dispersed in an equal volume of MilliQ water.

Dye incubation measurements

Hydrogels were prepared using the appropriate method as described above. For the anionic Fmoc-DDFF, the peptide was dissolved in aqueous sodium hydroxide (0.1 M) and MilliQ water at a concentration of 1% (w/v) before the addition of glucono-δ-lactone. Before gelation occurred, an equal volume of 100 μM dye solution was added, giving a final concentration of 50 μM dye and 0.5% (w/v) hydrogel. For the cationic Fmoc-KKFF, the peptide was dissolved in a 100 μM solution of dye, before an equal volume of 1x PBS (pH 7.4), giving final concentrations of 50 μM dye and 0.5% w/v) hydrogel. The gels were left to set overnight.

The next day, 1 mL 1x PBS (pH 7.4) was added to the gels and 500 μL aliquots removed at 1, 2, 4, 6, 8, 12 and 24 hours. After each aliquot was removed, an equal volume of 1x PBS was added to the gel. Absorbance measurements were recorded on a Varian Cary 50 Bio UV-Visible spectrophotometer.

Cell viability measurements

Cytotoxicity measurements were performed using an Alamar Blue colorimetric assay on HEK-293T cells. Each experiment was repeated at least three times. Cells were passaged using standard cell culture procedures. Cells were detached with trypsin and centrifuged (1000 rpm for 3 min). The supernatant was removed and the cells resuspended in Dulbecco's Modified Eagle Medium (DMEM) at a concentration of 100,000 cells/mL. Cells were seeded at a concentration of 10,000 cells/well.

For solution cytotoxicity measurements, cells were seeded into a 96 well plate and incubated overnight to attach to the substrate. Peptides were dissolved in DMSO and then diluted in DMEM to their desired concentration, with a final DMSO concentration of 1% (v/v). Media was then aspirated from the cells and replaced with 100 μL of the dissolved peptide solution in triplicate. Cells were then incubated for 24 hours and 10 μL Alamar Blue added to the wells, followed by incubation for 4 hours. Control wells included no cells, no treatment and a negative control of 20% (v/v) DMSO. The absorbance at 570 nm and 596 nm was recorded using a BioRad Benchmark plate reader.

For contact cytotoxicity measurements, to a 96-well plate, 100 μL of gel was added in triplicate with their respective triggers and allowed to set overnight. Surrounding wells were supplemented with water to ensure hydration of the gels. Gels triggered with GdL were then incubated for 24 hours with PBS in order to buffer the gels and minimise the effects of any excess GdL. Cells were then seeded atop the hydrogels and incubated for 24 hours, before 10 μL Alamar Blue was added to the wells, followed by further incubation for 4 hours. Control wells included cell-free gels, no hydrogels and a negative control of 20% (v/v) DMSO. The absorbance at 570 nm and 596 nm was recorded using a BioRad Benchmark plate reader.

Tethered bilayer lipid membrane experiments

Formation of tethered bilayer lipid membranes (tBLMs) was achieved using pre-prepared tethered benzyl-disulfide (tetra-ethyleneglycol) n = 2 C_{20}-phytanyl tethers (DLP) and benzyl-disulfide-tetra-ethyleneglycol-OH spacers (TEGOH) in the ratio of 1:9, as described previously

(SDx Tethered Membranes Pty. Ltd., Australia).[1] To the tethering chemistry first layer was added 8 μL of a 3 mM solution of a mobile lipid-phase mixture of 1-palmitoyl-2-oleoylphosphatidylcholine (POPC) lipids (Sigma-Aldrich) dissolved in ethanol. After a 2 min incubation, a rapid solvent exchange was undertaken with a buffer consisting of 100 mM NaCl and 10 mM tris at pH 7.2 to form the self-assembled tBLM. Swept frequency AC electrical impedance spectroscopy using a TethaQuick electrical impedance spectrometer (SDx Tethered Membranes Pty. Ltd., Australia) was used to determine membrane conduction. For this, phase and impedance magnitude data was collected using a 50 mV peak-peak AC excitation (2000 Hz – 0.1 Hz). An equivalent circuit consisting of a Constant Phase Element (CPE) in series with a Resistor/Capacitor (RC) element representing the lipid membrane, and an extra resistor in series representing the NaCl/tris buffer, was used to fit the data. The CPE in this circuit represents the imperfect capacitance created by the chemically coated gold tethering electrode.[2] Data were fitted using a proprietary adaptation of a Levenberg–Marquardt fitting routine. Peptides were initially dissolved in water (for polar cationic tetrapeptides) or basic water (for polar anionic/neutral tetrapeptides) at a concentration of 1% (w/v) (approximately 10 mM) and diluted to the appropriate concentration using the NaCl/tris buffer described above.

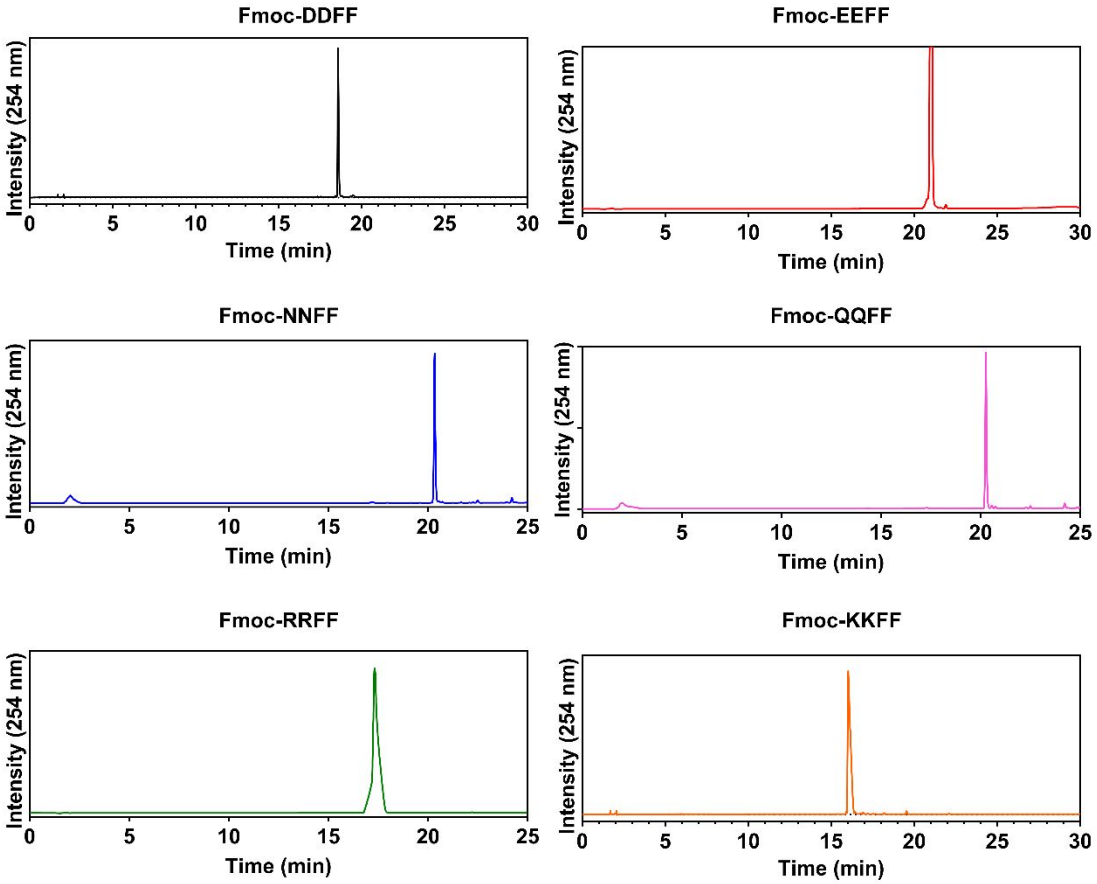

Fig. S1 – Analytical HPLC traces of polar tetrapeptides. Chromatrograms were performed at room temperature using a 5-95% acetonitrile gradient and a Waters XBridge BEH130 C_{18} 5 μm 4.6 × 150 mm column.

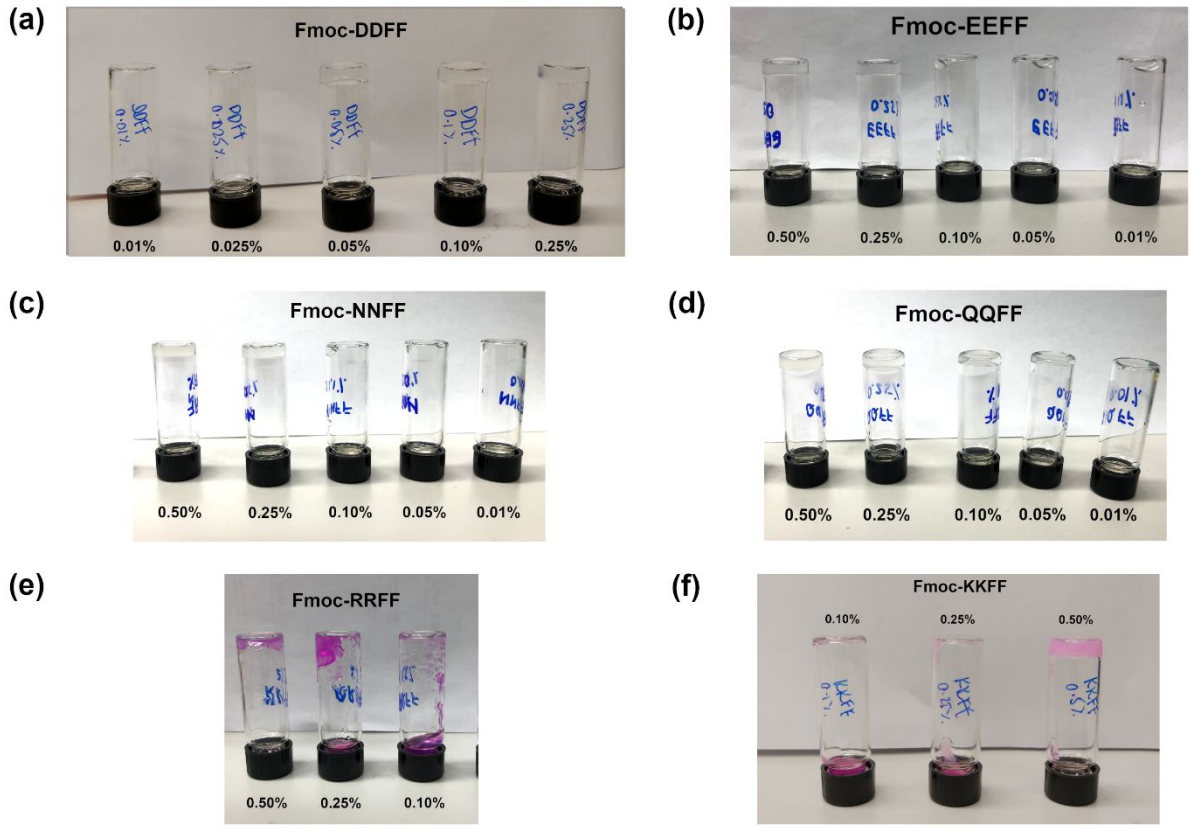

Fig. S2 – Minimum gel concentration tests for (a) Fmoc-DDFF, (b) Fmoc-EEFF, (c) Fmoc-NNFF, (d) Fmoc-QQFF, which were performed using the pH switch method described above. Minimum gel concentration tests for (e) Fmoc-RRFF and (f) Fmoc-KKFF were carried out via the aforementioned salt screening method.

Table S1. Fibre diameters measured for each polar tetrapeptide. A minimum of 20 nanofibres were measured across multiple AFM images.

Peptide	Fibre diameter (nm)
Fmoc-DDFF	5.5 ± 2.2
Fmoc-EEFF	6.5 ± 1.1
Fmoc-NNFF	2.8 ± 1.1
Fmoc-QQFF	6.4 ± 1.5
Fmoc-RRFF	6.1 ± 1.8
Fmoc-KKFF	4 ± 1.3

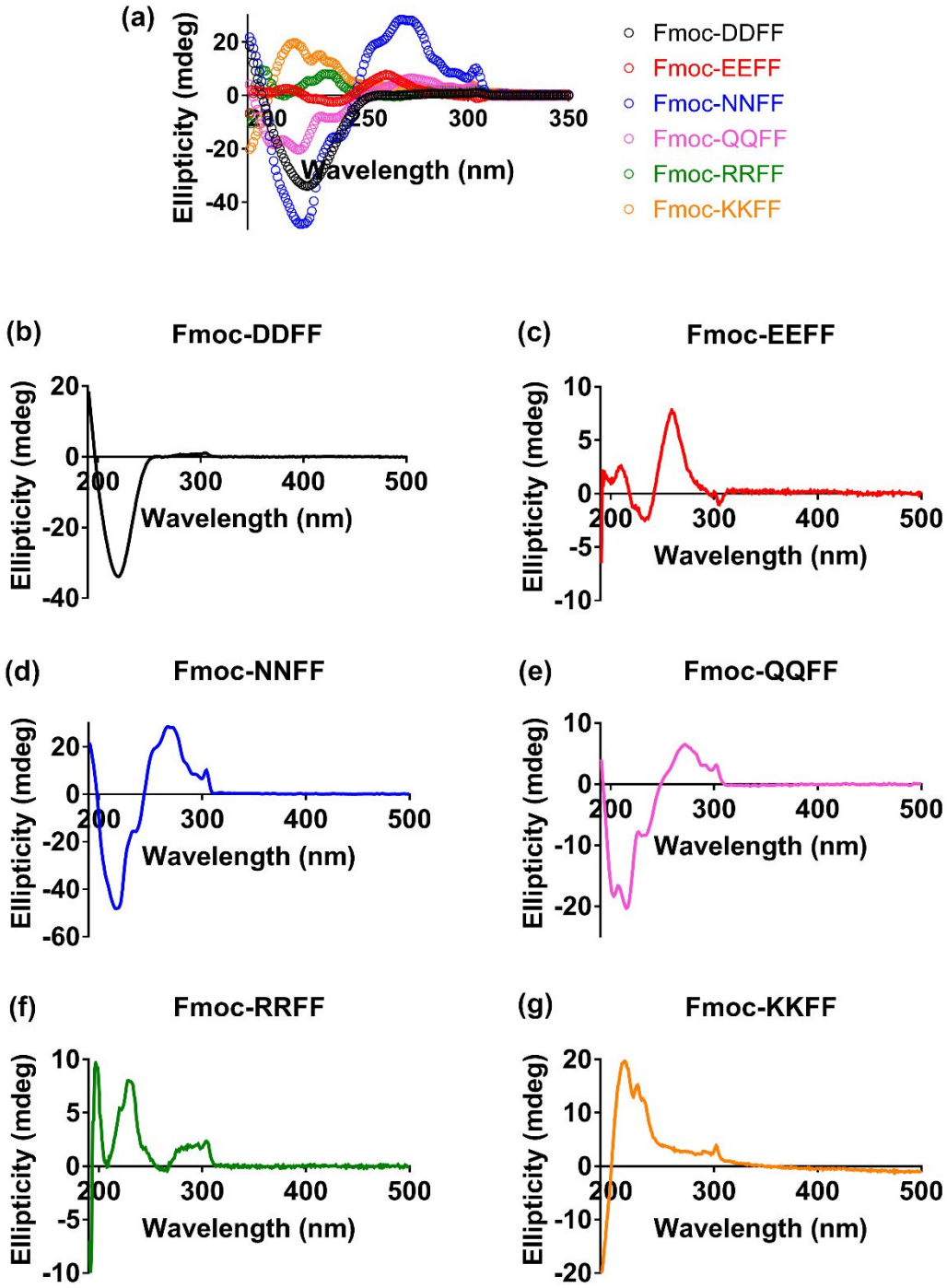

Fig. S3 – (a) overlaid and (b-g) individual CD spectra of polar tetrapeptide hydrogels formed using either pH switch method (Fmoc-DDFF, Fmoc-EEFF, Fmoc-NNFF, Fmoc-QQFF) or salt screen method (Fmoc-RRFF, Fmoc-KKFF) at 1% (w/v) and dispersed in MilliQ water to achieved a final concentration of 0.125% (w/v).

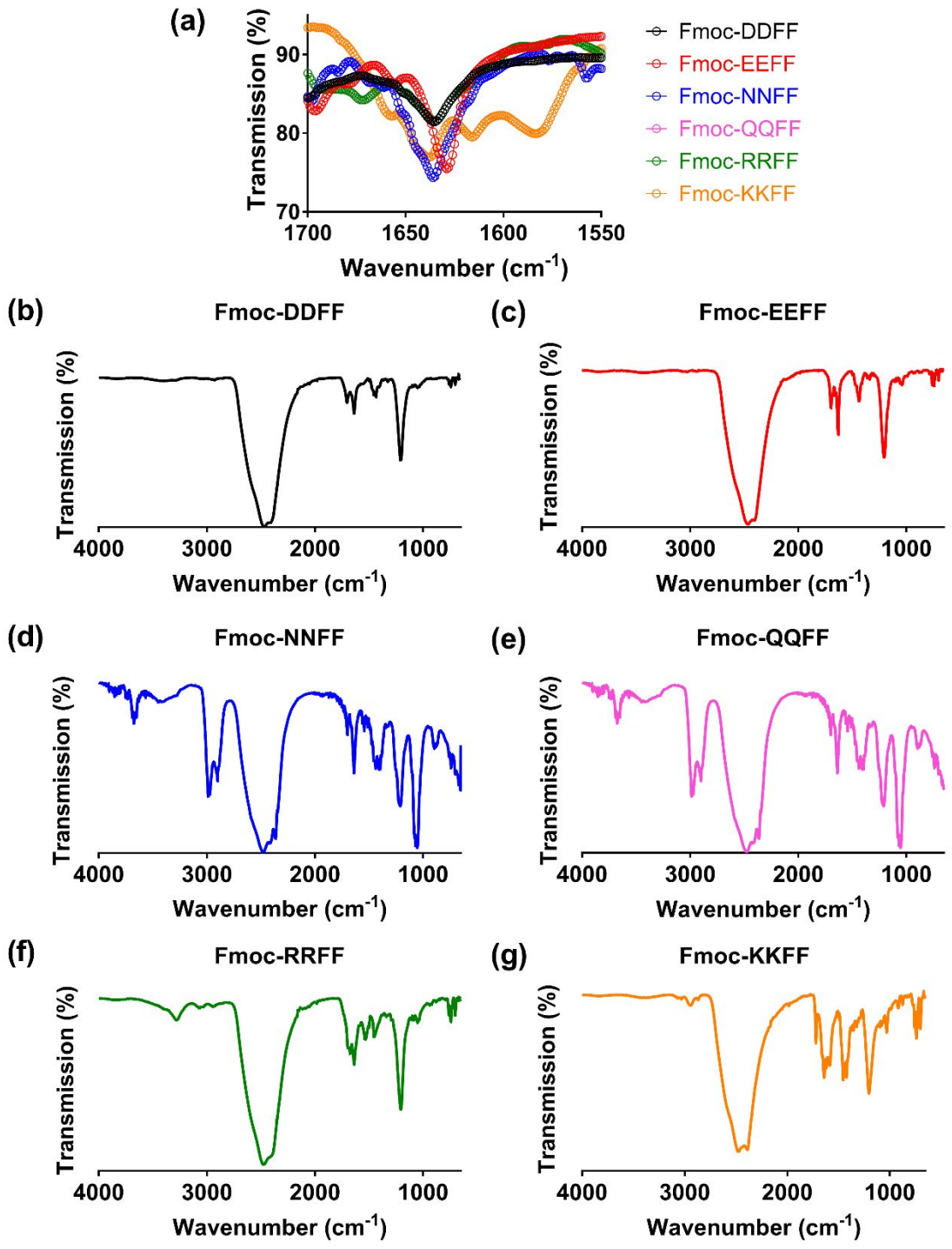

Fig. S4 – (a) Amide I region in the ATR-IR spectra of polar tetrapeptide hydrogels, full ATR-IR spectra of tetrapeptide hydrogels of (b) Fmoc-DDFF, (c) Fmoc-EEFF, (d) Fmoc-NNFF, (e) Fmoc-QQFF, (f) Fmoc-RRFF and (g) Fmoc-KKFF. Hydrogels were prepared at 1% (w/v) using the appropriate methodology in D_2O to avoid water O-H stretching vibrations at 1640 cm^{-1} which interfere with the Amide I region of the peptides.

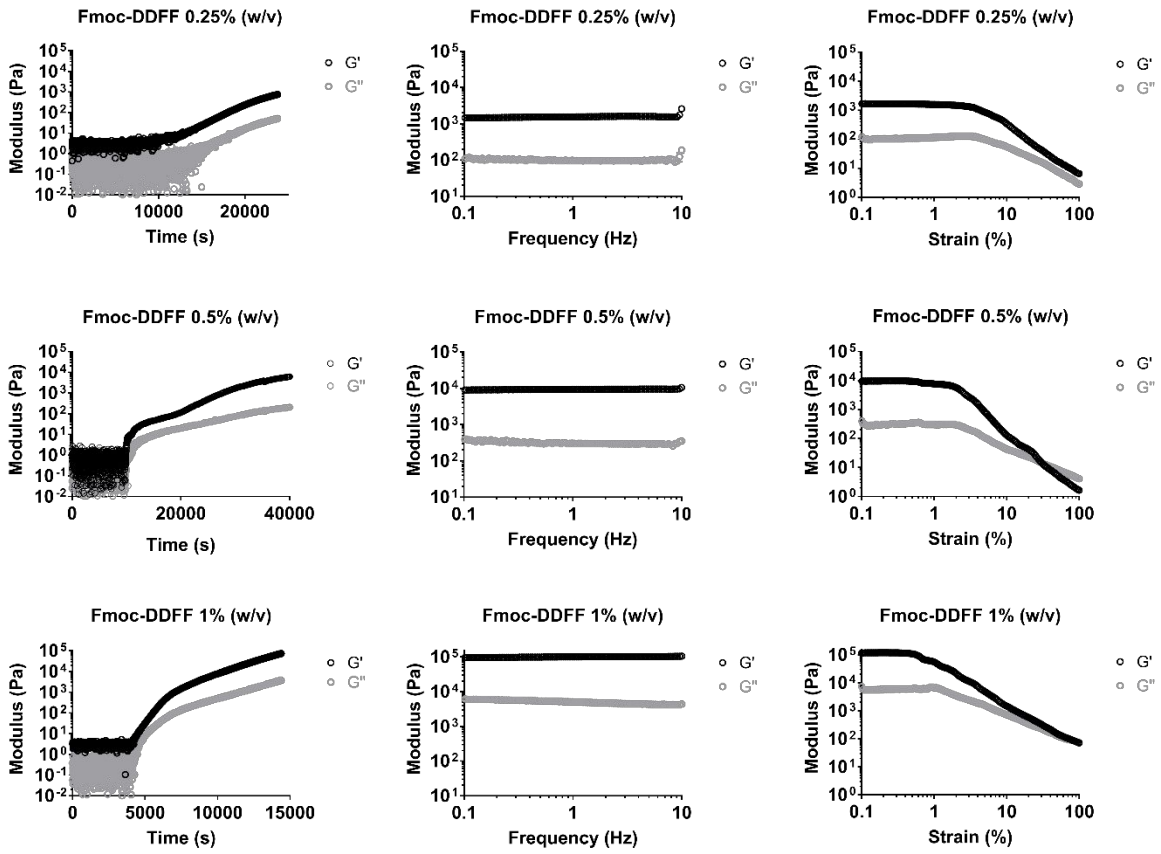

Fig. S5 – Rheological characterisation of Fmoc-DDFF at (top) 0.25% (w/v), (middle) 0.5% (w/v) and (bottom) 1% (w/v), reflecting the concentrations used in contact cytotoxicity measurements. Measurements consist of (left column) time resolved rheology (f = 1 Hz and γ = 0.2%), (middle column) frequency sweep (f = 0.1-10 Hz and γ = 0.2%) and (right column) strain sweep (f = 1 Hz and γ = 0.1-100%). All measurements were performed at 25 °C.

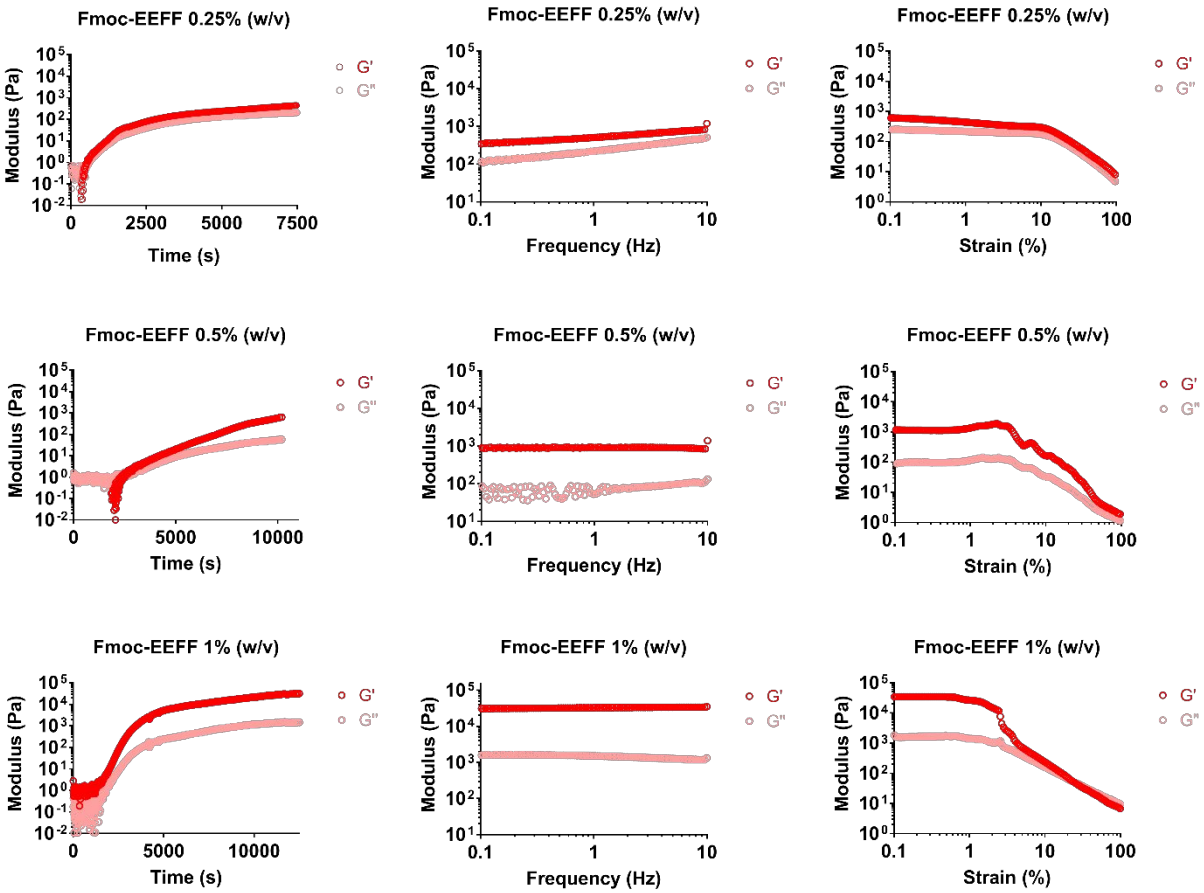

Fig. S6 – Rheological characterisation of Fmoc-EEFF at (top) 0.25% (w/v), (middle) 0.5% (w/v) and (bottom) 1% (w/v), reflecting the concentrations used in contact cytotoxicity measurements. Measurements consist of (left column) time resolved rheology (f = 1 Hz and γ = 0.2%), (middle column) frequency sweep (f = 0.1-10 Hz and γ = 0.2%) and (right column) strain sweep (f = 1 Hz and γ = 0.1-100%). All measurements were performed at 25 °C.

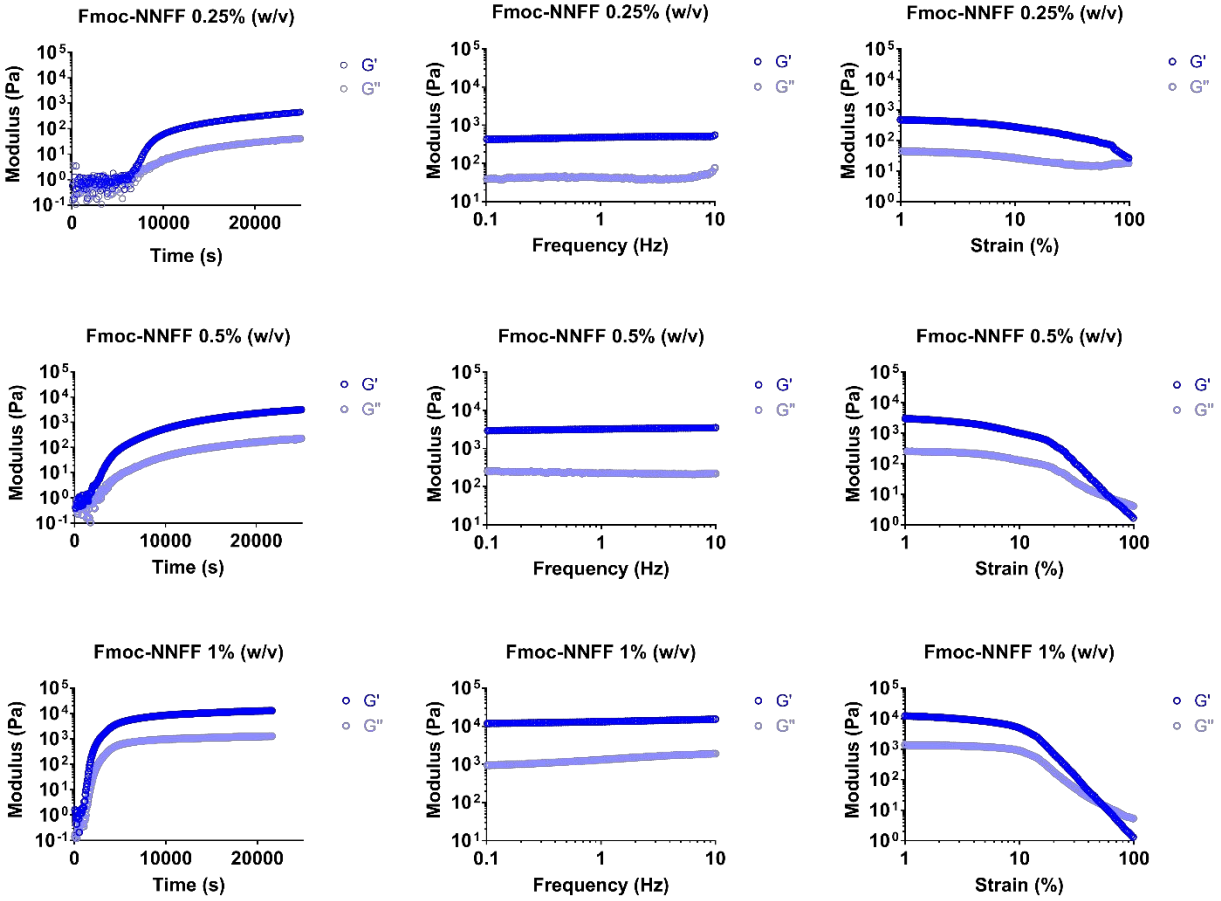

Fig. S7 – Rheological characterisation of Fmoc-NNFF at (top) 0.25% (w/v), (middle) 0.5% (w/v) and (bottom) 1% (w/v), reflecting the concentrations used in contact cytotoxicity measurements. Measurements consist of (left column) time resolved rheology (f = 1 Hz and γ = 0.2%), (middle column) frequency sweep (f = 0.1-10 Hz and γ = 0.2%) and (right column) strain sweep (f = 1 Hz and γ = 1-100%). All measurements were performed at 25 °C.

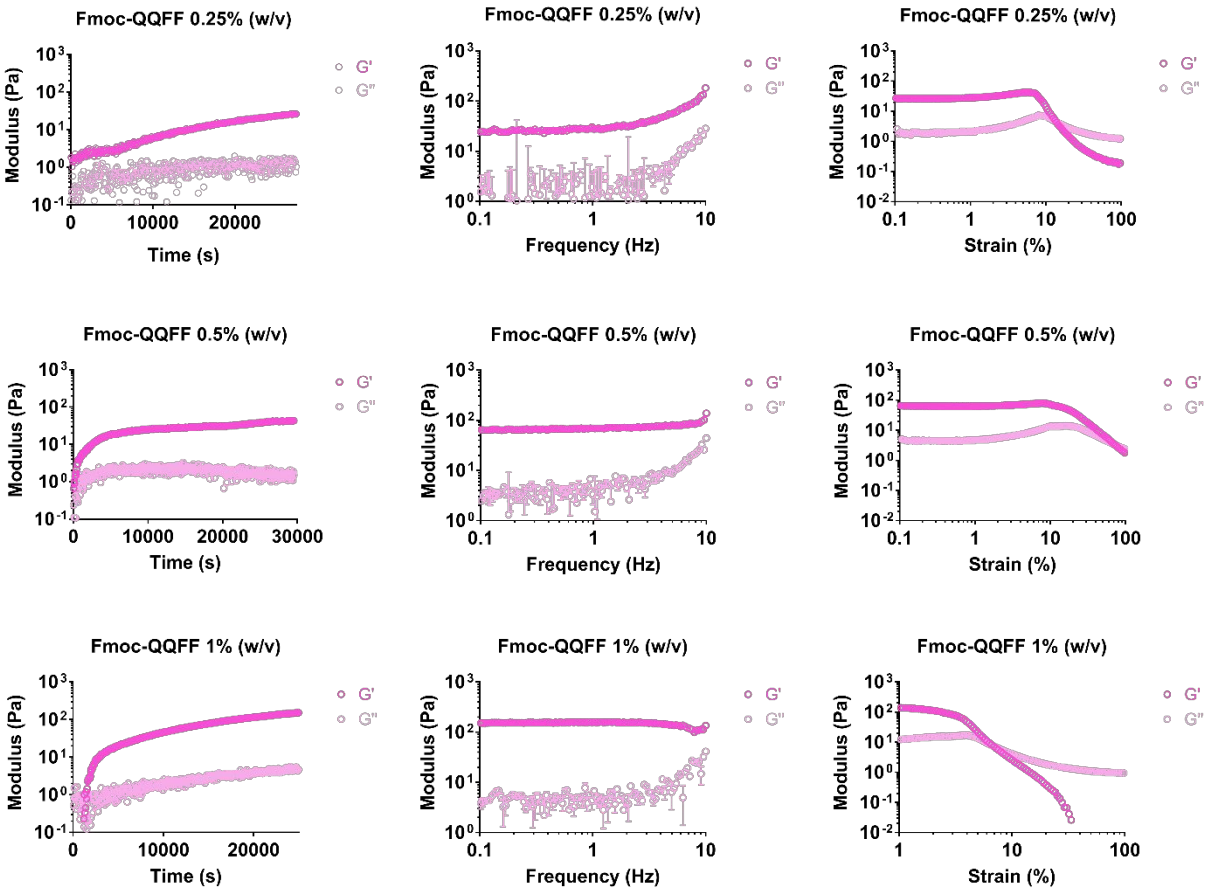

Fig. S8 – Rheological characterisation of Fmoc-QQFF at (top) 0.25% (w/v), (middle) 0.5% (w/v) and (bottom) 1% (w/v), reflecting the concentrations used in contact cytotoxicity measurements. Measurements consist of (left column) time resolved rheology (f = 1 Hz and γ = 0.2%), (middle column) frequency sweep (f = 0.1-10 Hz and γ = 0.2%) and (right column) strain sweep (f = 1 Hz and γ = 0.1-100%). All measurements were performed at 25 °C.

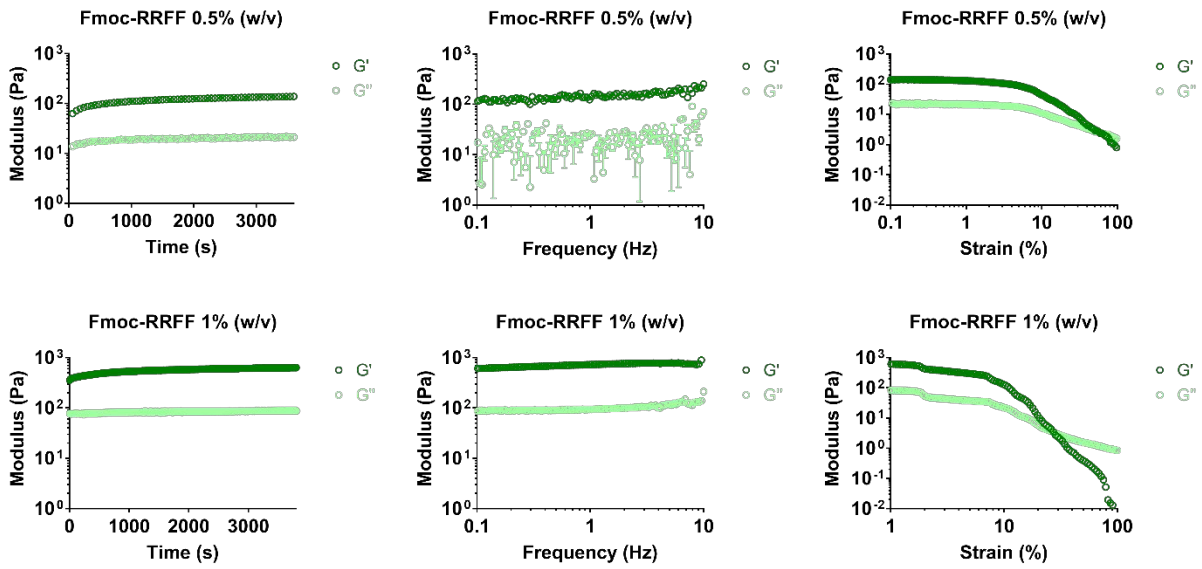

Fig. S9 – Rheological characterisation of Fmoc-RRFF at (top) 0.5% (w/v) and (bottom) 1% (w/v), reflecting the concentrations used in contact cytotoxicity measurements. Measurements consist of (left column) time resolved rheology (f = 1 Hz and γ = 0.2%), (middle column) frequency sweep (f = 0.1-10 Hz and γ = 0.2%) and (right column) strain sweep (f = 1 Hz and γ = 0.1-100%). All measurements were performed at 25 °C.

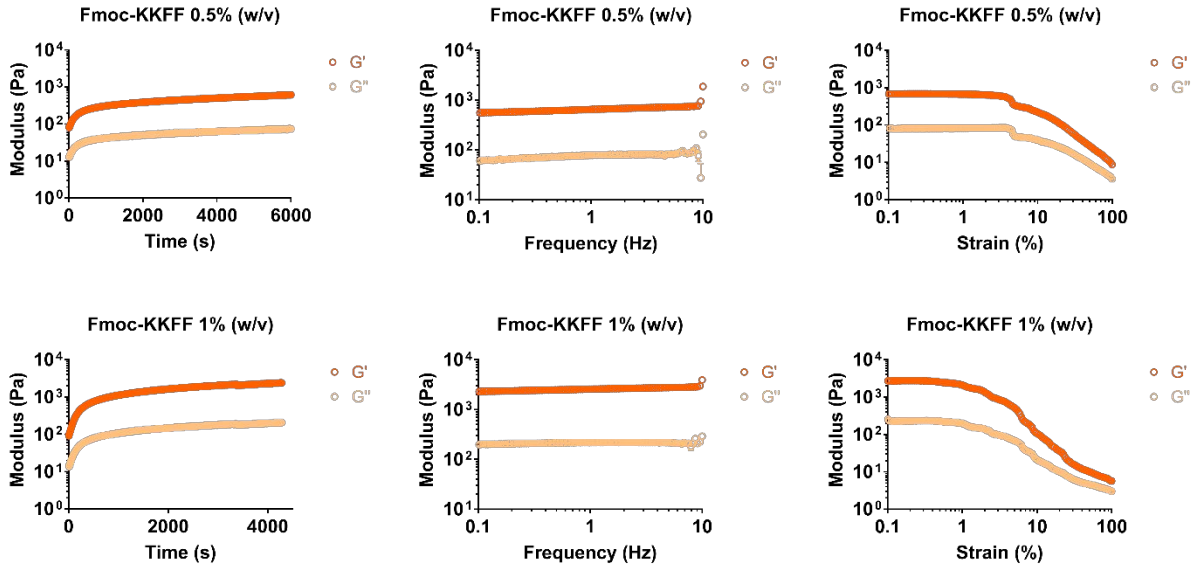

Fig. S10 – Rheological characterisation of Fmoc-KKFF at (top) 0.5% (w/v) and (bottom) 1% (w/v), reflecting the concentrations used in contact cytotoxicity measurements. Measurements consist of (left column) time resolved rheology (f = 1 Hz and γ = 0.2%), (middle column) frequency sweep (f = 0.1-10 Hz and γ = 0.2%) and (right column) strain sweep (f = 1 Hz and γ = 0.1-100%). All measurements were performed at 25 °C.

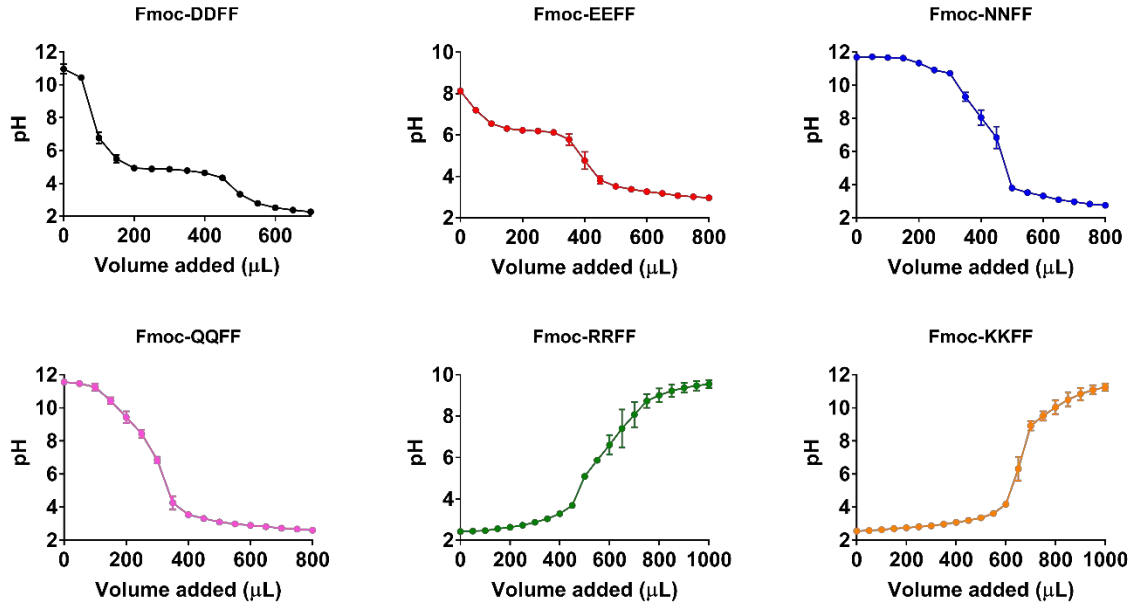

Fig. S11 – pK_a and pK_b determination for polar tetrapeptides. Polar anionic and neutral tetrapeptides were dissolved using 0.1 M NaOH and MilliQ water and 50 µL aliquots of 0.1 M HCl added. Polar cationic peptides were dissolved using 0.1 M HCl and MilliQ water and 50 µL aliquots of 0.1 M NaOH added. Experiments were repeated at least three times. Equivalence points were determined through plotting the first derivative of the graph.

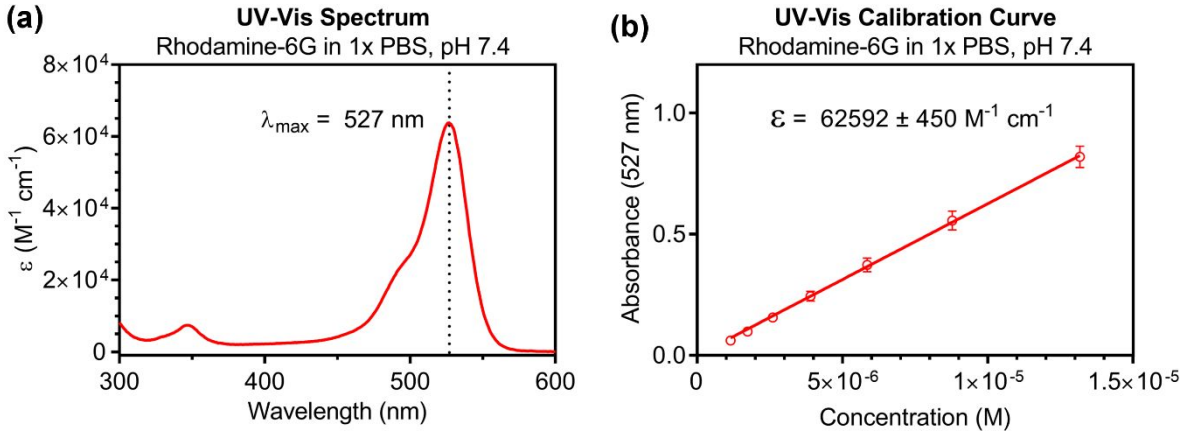

Fig. S12 – UV-Visible spectrum of (a) Rhodamine 6G and (b) associated calibration curve with calculated extinction coefficient.

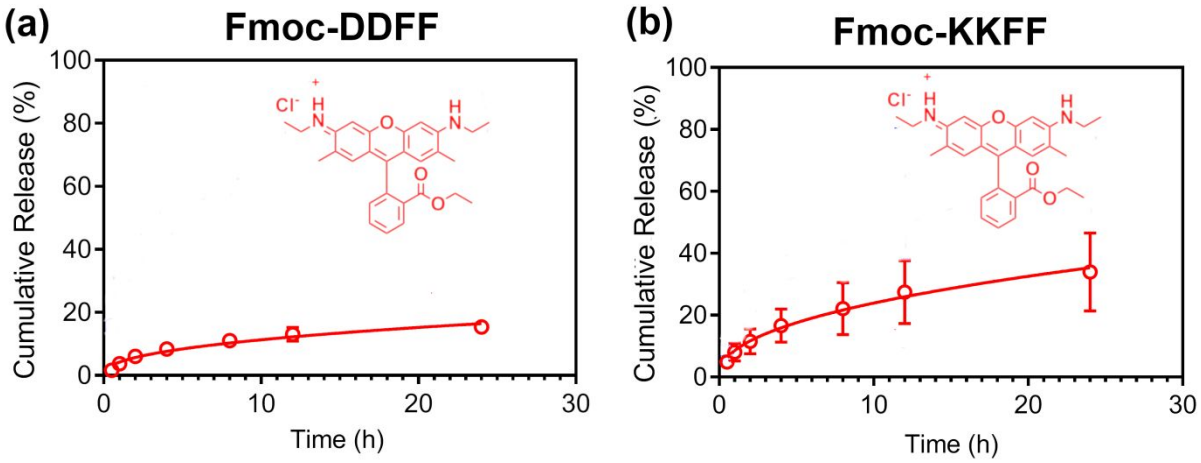

Fig. S12 – Release of positively charged Rhodamine 6G fluorophore (inset) from hydrogels of (a) negatively charged Fmoc-DDFF and (b) positively charged Fmoc-KKFF. Hydrogels were prepared at 1% (w/v) and total release after 24 h was approximately 17% for Fmoc-DDFF and 31% for Fmoc-KKFF, suggesting that peptide charge is conserved in the gel state.

References

1. C. G. Cranfield, S. Carne, B. Martinac. B. Cornell, *Methods in Molecular Biology (Methods and Protocols)*, **1232**, Humana Press, New York, 2015.

2. T. Berry, D. Dutta, R. Chen, A. Leong, H. Wang, W. A. Donald, M. Parviz, B. Cornell, M. Wilcox, N. Kumar, C. G. Cranfield, *Langmuir*, 2018, **34**,11586-11592.